

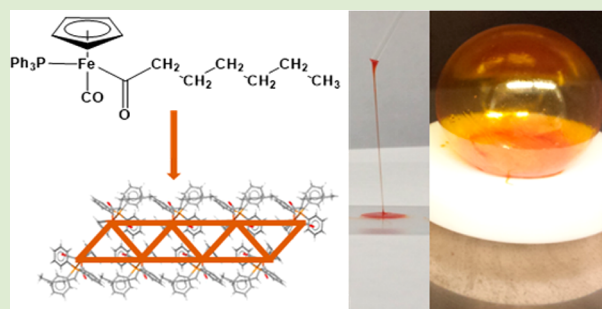
# Intermolecular Interactions of $\text{CpFePPh}_3(\text{CO})\text{CO}(\text{CH}_2)_5\text{CH}_3$ : From a Crystalline Solid to a Supramolecular “Iron-Truss” Polymer

Nicholas Lanigan, Abdeljalil Assoud, and Xiaosong Wang\*

Department of Chemistry and Waterloo Institute for Nanotechnology, University of Waterloo, 200 University Avenue West, Waterloo, Ontario N2L 3G1, Canada

## S Supporting Information

**ABSTRACT:**  $\text{PPh}_3\text{CpFe}(\text{CO})\text{CO}(\text{CH}_2)_5\text{CH}_3$  (FpC6) spontaneously forms supramolecular polymers in the solid state. The polymers crystallize slowly over a period of one month and can be recovered by melting the crystals at 65 °C. The rheological profile of FpC6 fits the Maxwell model indicating the presence of chain entanglement. Crystal analysis reveals that FpC6 is able to assemble, via cooperative  $\pi$ - $\pi$  interactions and weak C-H...O hydrogen bonding, into a duplex chain structure with truss arrangement of iron atoms. Powder X-ray diffraction (PXRD) of the polymers shows a double-peak pattern, characteristic for duplex ladder polymers. FTIR/ATR analysis further supports that carbonyl groups are involved in C-H...O hydrogen bonding responsible for the self-assembly. This discovery opens up new design motifs for organometallic supramolecular polymers.



Understanding and making use of intermolecular interactions in the solid state represents a major challenge in the application of functional materials, including organic electronics,<sup>1</sup> biological<sup>2</sup> and smart materials.<sup>3–5</sup> Crystal engineering is an effective approach for the study of molecular packing modes and has been used to explicitly elucidate intermolecular interactions,<sup>6–8</sup> such as hydrogen bonding and  $\pi$ - $\pi$  interactions.

Using well-understood noncovalent bonding, molecules have been designed with strong unidirectional intermolecular interactions for the construction of one-dimensional random coils analogous to covalent polymers or shape persistent nano-objects.<sup>9,10</sup> These assemblies are known as supramolecular polymers.<sup>10</sup> One of the first examples of this material is based on quadruple hydrogen bonding using ureidopyrimidinone (UPy) difunctional monomers.<sup>11,12</sup> Polymer behavior of the molecules was observed in both solution and solid. Following this initial work, a number of noncovalent motifs other than hydrogen bonding, such as  $\pi$ - $\pi$ ,<sup>13–15</sup> ionic,<sup>16</sup> and host-guest interactions,<sup>17–19</sup> have been explored for supramolecular polymerization. This has resulted in a broad range of functional supramolecular polymers.<sup>10</sup> Also, it is commonly observed that different types of interactions work synergistically, creating strong intermolecular forces for the creation of novel supramolecular polymers.<sup>20,21</sup> From crystal analysis of supramolecular polymer systems, multiple weak interactions (e.g., C-H...Cl, C-H...O)<sup>22</sup> working in concert with other interactions (e.g., solvophobic forces and  $\pi$ - $\pi$  interactions) are able to generate sufficient intermolecular attraction to generate supramolecular polymers.<sup>23,24</sup> Most supramolecular polymers are obtained via either isodesmic or nucleation-growth polymerization in solvents.<sup>9</sup> Solid-state supramolecular

polymerization is uncommon<sup>9</sup> but desirable, e.g., in the context of green chemistry and solid-state applications.

In addition to organic monomers,<sup>9</sup> metal coordination and organometallic molecules have attracted increasing attention for use in supramolecular polymerization because they offer additional intermolecular interactions, such as metal coordination<sup>25,26</sup> or metal-metal interaction.<sup>27–29</sup> They also incorporate metal species into the polymers which can impart different functionality including optical,<sup>29–32</sup> electrical,<sup>33</sup> and redox.<sup>34,35</sup> Moreover, the three-dimensional geometries of metal coordination building blocks offer a further possibility for polymer topologies and architecture design.<sup>36–38</sup> Although most supramolecular polymers are built from small molecules, it is worthy of note that one-dimensional structures can be assembled from organometallic PFS (PFS: polyferrocenylsilane) block copolymer in a controlled fashion.<sup>39</sup> This discovery has led to a new research topic of living self-assembly for precise synthesis and architecture design.<sup>33,40,41</sup> Most research using organometallic monomers is still based on a phenomenological approach. Very often there is no explicit elucidation of the chain structure responsible for the observed macromolecular behavior.<sup>42</sup> Exploring and understanding intermolecular interactions for chain construction has therefore become a crucial issue of the field and is essential for the future rational design of supramolecular organometallic polymers.

Synthesis of ladder-like oligomers and polymers, where two parallel macromolecular chains are connected via covalent

Received: October 17, 2014

Accepted: December 4, 2014

Published: December 8, 2014

interchain linkages, marks a state-of-the-art progress in synthetic chemistry.<sup>43–45</sup> Synthesis of this type of duplex supramolecular polymers via noncovalent interactions from small molecules has not been realized.

Herein we wish to report the first example of double-stranded duplex supramolecular polymer using iron-containing FpC6 (FpC6: CpFePPh<sub>3</sub>(CO)CO(CH<sub>2</sub>)<sub>5</sub>CH<sub>3</sub>) as the monomeric units. The polymerization of FpC6 occurs spontaneously in the solid state as a metastable structure that eventually crystallizes over a period of one month. The polymer can be recovered by melting the crystals at 65 °C. The rheological profile of FpC6 fits to the Maxwell model confirming the presence of chain entanglement. Crystal analysis of the molecules suggests that both  $\pi$ – $\pi$  interactions and weak C–H...O hydrogen bonding are cooperatively responsible for the duplex chain construction. The iron elements within the chain are spatially arranged into fused triangles resembling a bridge truss. We therefore name FpC6 a supramolecular “iron-truss” polymer.

FpC6, shown in Figure 1a, was prepared via migration insertion reaction (MIR) of CpFe(CO)<sub>2</sub>(CH<sub>2</sub>)<sub>5</sub>CH<sub>3</sub> in the presence of PPh<sub>3</sub>. During the synthesis and purification, it was observed that FpC6 exhibited solid-state behavior reminiscent of a polymeric material. After the solvent was removed, FpC6 formed a film along the sidewall of the round-bottom flask, and a glass-like solid remained at the bottom of the flask. Over a period of two months, the red glassy substance became a bright orange powder. The original glassy red solid can be recovered by heating the orange powder at 65 °C (Figure 1b). Fibers can be drawn from the melts of FpC6 using a glass rod (Figure 1c). When a freshly melted sample was placed in a vacuum oven the material ballooned (Figure 1d), suggesting that a free-standing film could be obtained. Formation of fiber and film is considered as a characteristic feature for polymer systems.

To confirm the presence of polymer chains, rheological experiments were performed. A typical result is shown in Figure 2. At low frequencies, the loss modulus  $G''$  of FpC6 is larger than the storage modulus  $G'$ , suggesting that FpC6 behaves like a viscous liquid. As the frequency increases, the storage modulus  $G'$  increases until it surpasses  $G''$  and eventually reaches a well-defined plateau. Despite some deviation at high frequencies, the experimental results can be fitted to the Maxwell model which describes the behavior of viscoelastic liquids with chain entanglement.<sup>46</sup> This result confirms the existence of FpC6 self-assembled chains. The plateau modulus,

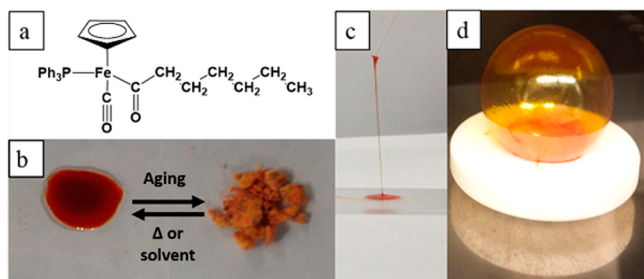


**Figure 1.** (a) Chemical structure of FpC6. (b) An orange crystalline powder could be obtained after aging the material for a period of one month. The amorphous glassy solid could be recovered by heating at 65 °C. (c) Fiber drawn from a melt of FpC6. (d) Bubble formed in a vacuum oven at 50 °C at –25 in. Hg from a film placed on a Teflon disk.

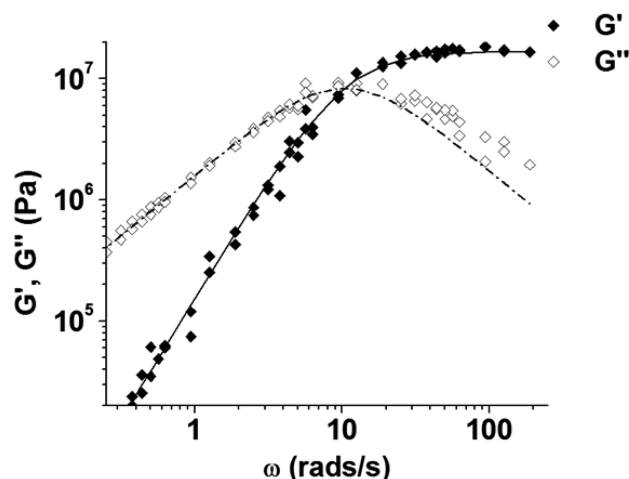


**Figure 2.** (a) Storage modulus  $G'$  ( $\blacklozenge$ ) and loss modulus  $G''$  ( $\diamond$ ) versus frequency for FpC6 at 17 °C. The solid and dotted curves represent the fit according to the Maxwell model of the storage and loss modulus, respectively.

$G_0$ , and the relaxation time,  $\tau$ , extracted from the experimental data using the Maxwell model are 16.8 MPa and 0.6 s, respectively.

Thermal analysis of FpC6 was performed using differential scanning calorimetry (DSC) and thermal gravimetric analysis (TGA). TGA indicates that there is no decomposition up to 135 °C (Figure S3, Supporting Information). DSC of an aged sample (Figure S4, Supporting Information) shows an endothermic peak starting at 57.2 °C corresponding to FpC6 melting temperature. The sample was subsequently cooled at a ramp of 10 °C/min. During this process, no recrystallization occurred, and a subtle glass transition is observed at 7.8 °C. When an amorphous sample is heated, a distinct glass transition occurs at 13.7 °C, but no crystallization or melting peaks are observed. The absence of  $T_c$  and  $T_m$  suggests that FpC6 is not able to crystallize on the time scale of the DSC experiment.

Powder X-ray diffraction (PXRD) was performed on the aged sample before and after heating at 65 °C. The freshly melted FpC6 is amorphous with two broad peaks centered at 11.78° and 20.34° (Figure 3a), similar to the PXRD pattern of silicon duplex polymers.<sup>47–49</sup> The origin of these two peaks corresponding to FpC6 polymer chain structure will be discussed later. After aging for 2 weeks and one month, PXRD was performed again on the same sample (Figure S5, Supporting Information). As shown in Figure S5 (Supporting Information), after 2 weeks, peaks appeared at higher X-ray scanning angles, suggesting ordered structures started to form at short distances. One month later, multiple peaks appeared at lower X-ray scanning angles, suggesting highly ordered crystalline structure was formed. The combination of DSC and PXRD experiments demonstrates that FpC6 supramolecular polymers are able to crystallize in bulk, but at a slow rate.

In order to determine the possible intermolecular interactions responsible for the chain structure, attempts have been made to obtain single crystals suitable for X-ray diffraction. Using a solvent mixture of 85% ethanol and 15% water, a single crystal was obtained which confirmed successful synthesis (see Supporting Information). However, the simulated diffraction pattern of the single crystal is different from the PXRD spectrum of FpC6 crystalline solid, suggesting that the packing

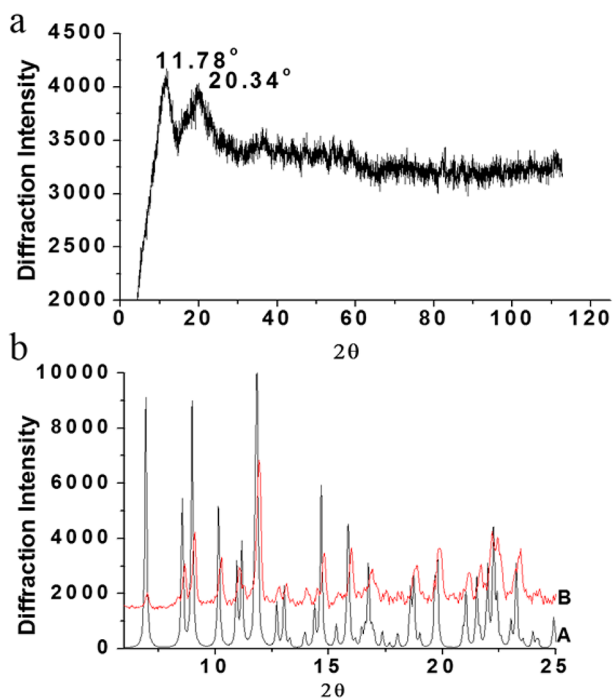


**Figure 3.** (a) Powder X-ray diffraction pattern of freshly melted FpC6. Two distinct peaks are observed at 11.78° and 20.34° corresponding to distances of approximately 7.5 and 4.4 Å. (b) Comparison of a simulated diffractogram from the single-crystal structure (A) to the diffractogram from the FpC6 aged for 2 months (B).

modes for FpC6 in crystalline solid and the single crystal obtained from ethanol/water mixture are not the same. In the case when FpC6 was recrystallized in hexane, a single crystal with the *Fdd2* space group was obtained (see Supporting Information). The simulated PXRD pattern from this single crystal is almost identical to that obtained from FpC6 crystalline powder (Figure 3b). This comparison indicates that FpC6 supramolecular polymers crystallized in solid into the *Fdd2* space group. As a result, crystal analysis of the *Fdd2* single crystal offers an opportunity to elucidate intermolecular interactions within the FpC6 crystalline powder. The analysis

results are listed in Figure 4. Short contact analysis starting from a single molecule revealed a parallel displaced  $\pi$ - $\pi$  interaction (Figure 4a), which has a distance of 3.9 Å from centroid to centroid. The distance between the cyclopentadienyl rings where they overlap is 3.3 Å. This forms a FpC6 dimer consisting of two nonsuperimposable isomers. Subsequently, this dimer acts as a monomer as it bonds to another FpC6 dimer through four C-H $\cdots$ O (2.595–2.746 Å) hydrogen bonds (Figure 4b). Following this pattern, a one-dimensional structure can be formed in the *c*-direction (Figure 4c). By connecting the iron atoms in the chain along the *c*-direction, a fused triangle configuration is revealed (Figure 4c and Figure S6, Supporting Information), which is analogous to a bridge-truss.

When viewed along the *c*-direction (Figure S7, Supporting Information), a unit cell consists of 16 chain cross sections. In the *b*-direction there are two C-H $\cdots$ O (2.627 Å) hydrogen bonds per monomer (FpC6 dimer) which extend from one chain to another (Figure S7, Supporting Information), while in the *a*-direction, there are no other interactions aside from van der Waals interactions. This analysis reveals that all interactions within the crystal structure, except two weak hydrogen bonds per monomer unit (*b*-direction), are involved in forming the chain structures in the *c*-direction. The chain-forming interactions are therefore comparatively stronger than interactions in other directions in the crystal. Meanwhile, the thermal energy of the alkyl chain is very high compared to the rest of the molecule (Figure 4d). The motion of the alkyl chains would then disrupt the interchain weak hydrogen bonds (*b*-direction). Consequently, FpC6 molecules are able to spontaneously associate into chains, which entangle each other resulting in polymer behavior of the molecules. The parallel alignment of multiple FpC6 chains into three-dimensional crystals, unlike the chain-folding mechanism for conventional crystalline polymers, is a slow process as confirmed by DSC and PXRD. At the melting temperature, the crystal structure would be disrupted, but FpC6 chain structures remain intact due to relatively stronger intermolecular interaction along the *c*-direction.

FpC6 supramolecular polymers with truss arrangement of iron elements are further supported by PXRD. As shown in

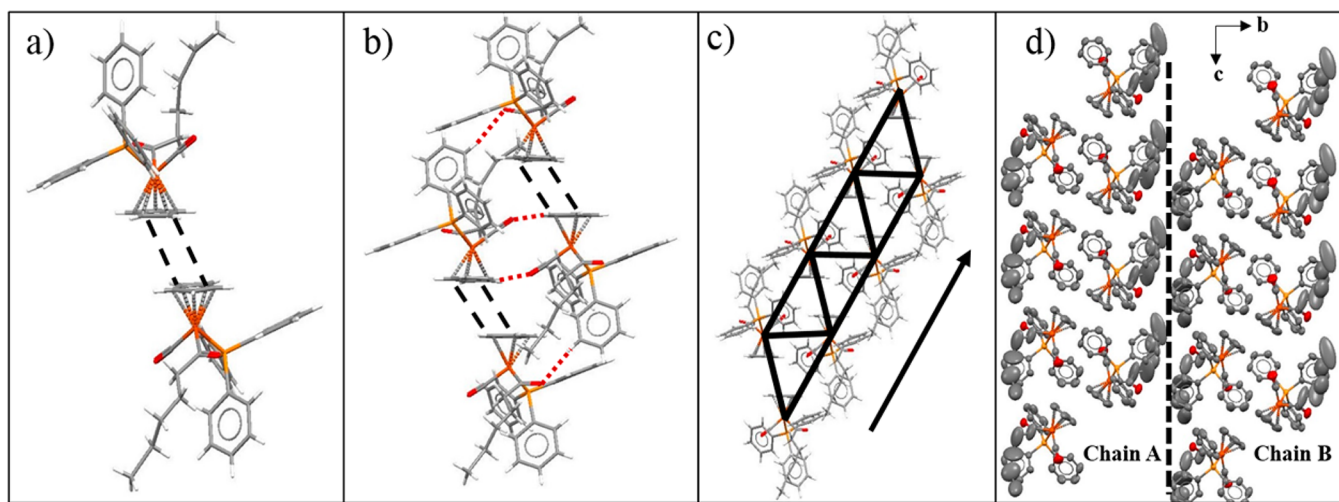


**Figure 4.** (a) Monomer formed by a parallel displaced  $\pi$ - $\pi$  interaction, drawn in black, between the cyclopentadienyl rings. (b) Dimer formed by four C-H $\cdots$ O hydrogen bonds, drawn in red, between 2 monomers. (c) Chain formed by four monomers. Arrow indicates *c*-axis and chain direction. (d) Two chains side by side in the single-crystal structure shown as thermal ellipsoids at a 50% probability level.



Figure 3a, the diffractogram of freshly melted FpC6 has a distinct peak at  $11.78^\circ$  and a broad peak at  $20.34^\circ$ , corresponding to distances of approximately 7.5 and 4.4 Å, respectively. This PXRD pattern bears a striking resemblance to the diffractograms reported for silicon covalent duplex chains and polysilsesquioxanes and has been considered as the characteristic PXRD pattern for duplex polymers.<sup>47–49</sup> For polysilsesquioxanes, the two peaks in the PXRD pattern are attributed to the inter rail spacing of the ladder and the distance between the duplex chains.<sup>47–49</sup> For the FpC6 supramolecular polymers, the average distance of the four iron atoms in the bridge truss is 7.44 Å (Figure S6, Supporting Information) which corresponds almost exactly to the first peak at 7.5 Å. This suggests that the first peak in the FpC6 PXRD pattern can be attributed to the inter truss distance analogous to polysilsesquioxanes. The second broad peak centered at  $20.34^\circ$  (4.4 Å) can in part be attributed to the presence of  $\pi$ – $\pi$  interactions between the Cp in FpC6 molecules (ca. 3.9 Å).<sup>50,51</sup> The broadness of the peaks could be caused by the flexibility of the chain which entangles and distorts some of the bonds. While each of these peaks in isolation is not conclusive evidence, the combination of the two peaks is exactly what is expected for a bridge-truss structure.

To further verify that C–H...O hydrogen bonds exist and are responsible for the elucidated supramolecular polymer chains and crystal structures (Figure 4b), FTIR/ATR of FpC6 amorphous and crystalline solid samples are compared to its solution in benzene (Figure S8, Supporting Information). For the solution sample, the absorption frequencies for the terminal and acyl carbonyl groups appear at 1911.5 and 1618.1  $\text{cm}^{-1}$ , respectively (Table S3, Supporting Information). These peak positions are considered to be associated with FpC6 molecules absent of significant hydrogen bonding. For the amorphous solid sample, these two frequencies shift to lower wavenumbers by 3 and 9  $\text{cm}^{-1}$  (Table S3, Supporting Information), supporting that both carbonyl groups are involved in the formation of hydrogen bonding<sup>52</sup> as expected from the structure of the chains (Figure 4). The magnitude of this decrease becomes greater once FpC6 is in a crystalline state (Table S3, Supporting Information), further supporting that the carbonyl groups play an important role in FpC6 supramolecular polymerization and crystallization via hydrogen bonding.

In summary, we have discovered that FpC6 organometallic molecules are able to self-assemble into a novel duplex supramolecular “iron-truss” polymer. The rheological profile of FpC6 clearly demonstrates the presence of long-range chain entanglement. The polymer is able to crystallize slowly and be recovered from the crystals by heating. Crystal analysis reveals that the duplex chain structure with truss arrangement of iron elements, similar to the ladder polymer of polysilsesquioxanes, is constructed via cooperative C–H...O hydrogen bonding and  $\pi$ – $\pi$  interactions. The chain structure resulting from the crystal analysis is supported by the characteristic PXRD double-peak pattern for duplex polymers and FTIR/ATR analysis. This discovery opens up new opportunities for supramolecular organometallic polymer design.

## ■ ASSOCIATED CONTENT

### Ⓢ Supporting Information

Experimental details, crystal analysis, TGA, DSC, time-resolved PXRD, and IR data. This material is available free of charge via the Internet at <http://pubs.acs.org>.

## ■ AUTHOR INFORMATION

### Corresponding Author

\*E-mail: [xiaosong.wang@uwaterloo.ca](mailto:xiaosong.wang@uwaterloo.ca).

### Author Contributions

The manuscript was written through contributions of all authors.

### Notes

The authors declare no competing financial interest.

## ■ ACKNOWLEDGMENTS

The Natural Sciences and Engineering Research Council of Canada (NSERC) and the University of Waterloo are acknowledged for financial support. We would like to acknowledge Professor Tam for providing access to the rheometer as well as Juntao Tang for his assistance in operating the rheometer. We also wish to thank Professor Duhamel and Professor Gauthier for their helpful discussions. In addition, we would like to thank Professor Stuart Rowan for his help correcting the manuscript.

## ■ REFERENCES

- (1) Henson, Z. B.; Muellen, K.; Bazan, G. C. *Nat. Chem.* **2012**, *4*, 699.
- (2) Morris, R. E.; Bu, X. *Nat. Chem.* **2010**, *2*, 353.
- (3) Desiraju, G. R. *Nature* **2001**, *412*, 397.
- (4) Wojtecki, R. J.; Meador, M. A.; Rowan, S. J. *Nat. Mater.* **2011**, *10*, 14.
- (5) Cordier, P.; Tournilhac, F.; Soulie-Ziakovic, C.; Leibler, L. *Nature* **2008**, *451*, 977.
- (6) Hollingsworth, M. D. *Science* **2002**, *295*, 2410.
- (7) Braga, D.; Brammer, L.; Champness, N. R. *CrystEngComm* **2005**, *7*, 1.
- (8) Desiraju, G. R. *Angew. Chem., Int. Ed.* **2007**, *46*, 8342.
- (9) De Greef, T. F. A.; Smulders, M. M. J.; Wolffs, M.; Schenning, A. P. H. J.; Sijbesma, R. P.; Meijer, E. W. *Chem. Rev.* **2009**, *109*, 5687.
- (10) Aida, T.; Meijer, E. W.; Stupp, S. I. *Science* **2012**, *335*, 813.
- (11) de Greef, T. F.; Meijer, E. *Nature* **2008**, *453*, 171.
- (12) Sijbesma, R. P.; Beijer, F. H.; Brunsveld, L.; Folmer, B. J. B.; Hirschberg, J. H. K. K.; Lange, R. F. M.; Lowe, J. K. L.; Meijer, E. W. *Science* **1997**, *278*, 1601.
- (13) Haino, T.; Fujii, T.; Watanabe, A.; Takayanagi, U. *Proc. Natl. Acad. Sci. U.S.A.* **2009**, *106*, 10477.
- (14) Hill, J. P.; Jin, W.; Kosaka, A.; Fukushima, T.; Ichihara, H.; Shimomura, T.; Ito, K.; Hashizume, T.; Ishii, N.; Aida, T. *Science* **2004**, *304*, 1481.
- (15) Jin, W.; Yamamoto, Y.; Fukushima, T.; Ishii, N.; Kim, J.; Kato, K.; Takata, M.; Aida, T. *J. Am. Chem. Soc.* **2008**, *130*, 9434.
- (16) Sendai, T.; Biswas, S.; Aida, T. *J. Am. Chem. Soc.* **2013**, *135*, 11509.
- (17) Park, J. S.; Yoon, K. Y.; Kim, D. S.; Lynch, V. M.; Bielawski, C. W.; Johnston, K. P.; Sessler, J. L. *Proc. Natl. Acad. Sci. U.S.A.* **2011**, *108*, 20913.
- (18) Haino, T.; Watanabe, A.; Hirao, T.; Ikeda, T. *Angew. Chem., Int. Ed.* **2012**, *51*, 1473.
- (19) Huang, F.; Gibson, H. W. *J. Am. Chem. Soc.* **2004**, *126*, 14738.
- (20) Liu, Y.; Fang, R.; Tan, X.; Wang, Z.; Zhang, X. *Chem.–Eur. J.* **2012**, *18*, 15650.
- (21) Wackerly, J. W.; Moore, J. S. *Macromolecules* **2006**, *39*, 7269.
- (22) Rest, C.; Mayoral, M. J.; Fucke, K.; Schellheimer, J.; Stepanenko, V.; Fernández, G. *Angew. Chem., Int. Ed.* **2014**, *53*, 700.
- (23) Zhang, Z.; Luo, Y.; Chen, J.; Dong, S.; Yu, Y.; Ma, Z.; Huang, F. *Angew. Chem., Int. Ed.* **2011**, *50*, 1397.
- (24) Rest, C.; Martin, A.; Stepanenko, V.; Allampally, N. K.; Schmidt, D.; Fernandez, G. *Chem. Commun.* **2014**, *50*, 13366.
- (25) Enomoto, M.; Kishimura, A.; Aida, T. *J. Am. Chem. Soc.* **2001**, *123*, 5608.

- (26) Wurthner, F.; Stepanenko, V.; Sautter, A. *Angew. Chem., Int. Ed.* **2006**, *45*, 1939.
- (27) Mayoral, M. J.; Rest, C.; Stepanenko, V.; Schellheimer, J.; Albuquerque, R. Q.; Fernandez, G. *J. Am. Chem. Soc.* **2013**, *135*, 2148.
- (28) Sun, Y.; Ye, K.; Zhang, H.; Zhang, J.; Zhao, L.; Li, B.; Yang, G.; Yang, B.; Wang, Y.; Lai, S.-W.; Che, C.-M. *Angew. Chem., Int. Ed.* **2006**, *45*, 5610.
- (29) Chen, Y.; Cheng, G.; Li, K.; Shelar, D. P.; Lu, W.; Che, C.-M. *Chem. Sci.* **2014**, *5*, 1348.
- (30) Fukino, T.; Joo, H.; Hisada, Y.; Obana, M.; Yamagishi, H.; Hikima, T.; Takata, M.; Fujita, N.; Aida, T. *Science* **2014**, *344*, 499–504.
- (31) Wong, K. M.-C.; Yam, V. W.-W. *Acc. Chem. Res.* **2011**, *44*, 424.
- (32) Burnworth, M.; Tang, L.; Kumpfer, J. R.; Duncan, A. J.; Beyer, F. L.; Fiore, G. L.; Rowan, S. J.; Weder, C. *Nature* **2011**, *472*, 334.
- (33) Zhang, W.; Jin, W.; Fukushima, T.; Saeki, A.; Seki, S.; Aida, T. *Science* **2011**, *334*, 340.
- (34) Miller, A. K.; Li, Z.; Streltzyk, K. A.; Jamieson, A. M.; Rowan, S. *J. Polym. Chem.* **2012**, *3*, 3132.
- (35) Adhikari, B.; Afrasiabi, R.; Kraatz, H.-B. *Organometallics* **2013**, *32*, 5899.
- (36) Yan, X.; Li, S.; Pollock, J. B.; Cook, T. R.; Chen, J.; Zhang, Y.; Ji, X.; Yu, Y.; Huang, F.; Stang, P. J. *Proc. Natl. Acad. Sci. U.S.A.* **2013**, *110*, 15585.
- (37) Yan, X.; Jiang, B.; Cook, T. R.; Zhang, Y.; Li, J.; Yu, Y.; Huang, F.; Yang, H.-B.; Stang, P. J. *J. Am. Chem. Soc.* **2013**, *135*, 16813.
- (38) Yan, X.; Cook, T. R.; Pollock, J. B.; Wei, P.; Zhang, Y.; Yu, Y.; Huang, F.; Stang, P. J. *J. Am. Chem. Soc.* **2014**, *136*, 4460.
- (39) Wang, X.; Guerin, G.; Wang, H.; Wang, Y.; Manners, I.; Winnik, M. A. *Science* **2007**, *317*, 644.
- (40) Ogi, S.; Sugiyasu, K.; Manna, S.; Samitsu, S.; Takeuchi, M. *Nat. Chem.* **2014**, *6*, 188.
- (41) Anraku, Y.; Kishimura, A.; Yamasaki, Y.; Kataoka, K. *J. Am. Chem. Soc.* **2013**, *135*, 1423.
- (42) Lanigan, N.; Wang, X. *Chem. Commun.* **2013**, *49*, 8133.
- (43) Scherf, U. *J. Mater. Chem.* **1999**, *9*, 1853.
- (44) Luh, T.-Y. *Acc. Chem. Res.* **2012**, *46*, 378.
- (45) Gong, B. *Acc. Chem. Res.* **2012**, *45*, 2077.
- (46) Lortie, F.; Boileau, S.; Bouteiller, L.; Chassenieux, C.; Demé, B.; Ducouret, G.; Jalabert, M.; Lauprêtre, F.; Terech, P. *Langmuir* **2002**, *18*, 7218.
- (47) Andrianov, K. A.; Slonimsky, G. L.; Zhdanov, A. A.; Tsvankin, D. Y.; Levin, V. Y.; Papkov, V. S.; Kvachev, Y. P.; Belavtseva, E. M. *J. Polym. Sci., Polym. Chem. Ed.* **1976**, *14*, 1205.
- (48) Xinsheng, Z.; Lianghe, S.; Chaoran, H. *Chin. J. Polym. Sci.* **1987**, *5*, 353.
- (49) Liu, C.; Liu, Y.; Shen, Z.; Xie, P.; Zhang, R.; Yang, J.; Bai, F. *Macromol. Chem. Phys.* **2001**, *202*, 1581.
- (50) Zhang, J.-J.; Lu, W.; Sun, R. W.-Y.; Che, C.-M. *Angew. Chem., Int. Ed.* **2012**, *51*, 4882.
- (51) Sukul, P. K.; Asthana, D.; Mukhopadhyay, P.; Summa, D.; Muccioli, L.; Zannoni, C.; Beljonne, D.; Rowan, A. E.; Malik, S. *Chem. Commun.* **2011**, *47*, 11858.
- (52) Desiraju, G. R.; Steiner, T. *The weak hydrogen bond in structural chemistry and biology*; Oxford University Press: New York, 1999.